Journal of Plant Nutrition and Soil Science

WILEY-VCH

RESEARCH ARTICLE OPEN ACCESS

Clay Mineral–Hydrophobic Organic Compound Interactions in Miniaturized Adsorption Experiments: Exemplary Studies With Bentonites and Hexachlorobenzene

Leonard Böhm[1] | Peter Grančič[2] | Lilli P. Butzke[1] | Stephan Kaufhold[3] | Jan Siemens[1] | Daniel Tunega[2] | Martin H. Gerzabek[2]

[1]Institute of Soil Science and Soil Conservation, Research Centre for BioSystems, Land Use and Nutrition (iFZ), Justus Liebig University Giessen, Giessen, Germany | [2]Institute for Soil Research, Department of Forest and Soil Sciences, University of Natural Resources and Life Sciences Vienna, Vienna, Austria | [3]BGR, Bundesanstalt für Geowissenschaften und Rohstoffe, Hannover, Germany

Correspondence: Leonard Böhm (leonard.boehm@umwelt.uni-giessen.de)

Received: 27 March 2024 | **Revised:** 30 September 2024 | **Accepted:** 29 November 2024

Academic Editor: Karin Eusterhues

Funding: Funding was received from Deutsche Forschungsgemeinschaft 443637168, DFG BO5388/1-1, Austrian Science Fund I 4876-N.

Keywords: distribution coefficients (K_d) | layer charge density (LCD) | Milos bentonite | persistent organic pollutants (POP) | phyllosilicates | smectites | solid-phase microextraction (SPME) | Wyoming bentonite

ABSTRACT

Background: Hydrophobic organic compounds (HOCs) are ubiquitous in the environment. Especially halogenated HOCs can pose a major threat to human and environmental health. They show high affinity toward organic matter (OM), and adsorption processes are extensively investigated. Contrary, adsorption to minerals is often considered negligible, and knowledge on HOC interactions with clay minerals (CM) is still scarce.

Aims: We aimed to apply an optimized method for the straightforward and sensitive quantification of HOC–CM interactions in miniaturized systems to quantify hexachlorobenzene (HCB) adsorption to native bentonites and to evaluate the influence of different mineral characteristics on adsorption.

Methods: HOC–CM interactions were studied in miniaturized batch adsorption experiments with HCB as HOC representative and 21 native bentonites as CM phases. Additionally, five of the bentonites were used as sorbents after wet size fractionation (<2 μm) and homoionic cation exchange (Ca^{2+}). Linear adsorption isotherms and solid–liquid distribution coefficients K_d were calculated after HCB analysis by solid-phase microextraction (SPME) coupled to GC–MS.

Results: HCB adsorption to selected native bentonites showed a large variation over several orders of magnitude (log K_d 1.8–4.1). Size-fractionation and Ca^{2+}-modification tended to slightly decrease the K_d values compared to the five corresponding native bentonites (log K_d: 1.9–3.8 vs. log K_d: 2.0–4.1). Most promising parameters for explaining adsorption strength by different CM characteristics were layer charge density (LCD) and cation exchange capacity (CEC). However, no single factor could be attributed to explain the observed variability of adsorption. The miniaturized batch adsorption method reduces the required amounts of purified CM and toxic chemicals while providing excellent sensitivity and reproducibility.

Conclusions: HOC adsorption to native, smectite-rich bentonites is mostly moderate but can be as high as adsorption to pure OM phases for some bentonites. The variation in adsorption appears to be controlled by a combination of several factors that might include additional factors not previously considered, especially for the bentonites with the strongest adsorption of HCB.

1 | Introduction

Hydrophobic organic compounds (HOCs), such as halogenated aromatic hydrocarbons, can be highly persistent in the environment and cause harmful effects on humans and biota (Desforges et al. 2018; Starek-Świechowicz, Budziszewska, and Starek 2017). Despite being banned for decades, halogenated compounds are still ubiquitous in the environment. In addition to legacy persistent organic pollutant (POP) distribution in the environment, new knowledge is emerging about sources that have previously received little or no attention (Wiltschka et al. 2023). Hexachlorobenzene (HCB; Table S1), part of the first group of regulated POPs, was primarily used as a seed treatment agent and pesticide but was also unintentionally synthesized in various production processes and during incomplete waste incineration (Bailey 2001; Barber et al. 2005; United Nations Environment Programme 2020). In addition to the environmental occurrence of legacy concentrations, HCB is still emitted to the environment, mainly from fuel combustion and the metal industry. Starting from global emissions of about 23,000 kg HCB a^{-1} in the mid-1990s (Bailey 2001), emissions have decreased significantly since then (e.g., in Germany from 2000–3000 kg in the 1990s to <5 kg in 2022; UBA 2024). Nevertheless, HCB can still be found ubiquitously in the environment due to its persistence or rather slow elimination (Hites, Bidleman, and Venier 2022; Lohmann et al. 2023; Meijer et al. 2003; Pohlert et al. 2011). As a hydrophobic compound, HCB strongly interacts with nonpolar phases and therefore has a high potential for accumulation in the lipid tissues of organisms and a high affinity for sorption to organic matter (OM) in soils and sediments. Therefore, bioaccumulation and HOC–OM interactions have been extensively studied (Ahmed et al. 2015; Pan, Ning, and Xing 2008; Pouch, Zaborska, and Pazdro 2018; Schlechtriem et al. 2017). Compared to OM, the affinity of HOCs for mineral phases is usually lower or rather non-existent. Nevertheless, relevant adsorption of (moderately) nonpolar chemicals can also occur on mineral phases such as oxides (Mader, Goss, and Eisenreich 1997) and clay minerals (Awad et al. 2019; Hu et al. 2019; Jaynes and Boyd 1991; Liu et al. 2009; Qu et al. 2011; Sadri et al. 2018). For molecules with an aromatic system, proposed interaction mechanisms include hydrophobic interactions with uncharged mineral surfaces and charge-dependent interactions such as electron–π electron donor acceptor (n–π EDA) interactions, but also cation–π interactions (Böhm et al. 2023; Georgieva et al. 2023; Grančič et al. 2023; Jaynes and Boyd 1991; Pašalić et al. 2017; Pei et al. 2012; Qu et al. 2011). Despite the increasing number of studies, many open questions remain for HOC–CM interactions. Although several studies investigated interactions of hydrophobic compounds with mineral phases, these mainly reflected moderately hydrophobic and clearly water-soluble substances (e.g., in the range of log $K_{OW} \approx$ 2–3), such as benzene, monochlorobenzene, or naphthalene. Hence, data on the adsorption of highly hydrophobic compounds (log $K_{OW} >$ 5) to mineral phases in solid–liquid systems are scarce, especially in case of halogenated compounds from the group of POPs. In a previous study, we detected relevant HCB adsorption to various phyllosilicate minerals, among which smectites showed a large variation of HCB adsorption (Böhm et al. 2023). To the best of our knowledge, this study provided the first data on HCB adsorption to different (clay) minerals. However, data on HCB–bentonite adsorption are still missing, and the effect of compositional variation of smectite on the adsorption strength is not yet understood (Böhm et al. 2023). In addition to enhancing the understanding of basic mechanistic processes, providing systematic information on the adsorption characteristics of smectite-rich bentonites is also crucial from an application-oriented perspective: Bentonites are highly relevant in the management of contaminated sites, such as its use for landfill sealings, trench cutoff walls, or in the development of super adsorbents for water treatment. Knowledge regarding systematic variation in POP sorption to bentonites opens the possibility to optimize the protective function of bentonite sealings and the treatment of contaminated waters.

A potential explanation for the scarcity of studies and data on POP–CM interactions could be the former lack of analytical approaches allowing for sensitive analysis of trace concentrations (i.e., with relevant or rather maximum water-soluble concentrations often in the range of pg–µg L^{-1}) either in general or specifically in adsorption experiments. Although sensitivity and robustness of analytical instruments drastically increased over the last decades, sample extraction is still mainly based on solvents. In the context of adsorption experiments with test substances in trace concentrations, this may be associated with inherent drawbacks. For example, small or regular test systems conflict with low test substance concentrations but would lose relevance or even validity if concentrations are increased above environmentally relevant concentrations or even above maximum water solubility. On the other hand, large-scale approaches with high volume extractions would lead to enhanced labor intensity and further drawbacks during extraction such as the co-extraction of sample matrix or volatility losses during concentration of extracts. In case of highly hydrophobic compounds, such experiments would be either highly laborious or potentially unfeasible.

In contrast, the non-exhaustive solvent-free technique solid-phase microextraction (SPME) may allow sensitive analysis from small sample volumes in trace concentrations and selective extraction and differentiation between bound and freely dissolved molecule species (Arthur and Pawliszyn 1990; Bondarenko and Gan 2009; Heringa and Hermens 2003; Mayer et al. 2003; Poerschmann et al. 1997; Ouyang and Jiang 2016; Zhang and Pawliszyn 1993). Our previous work with SPME included the determination of adsorption coefficients as well as the determination of trace concentrations using internal standard correction (Böhm, Schlechtriem, and Düring 2016; Böhm et al. 2017; Böhm

et al. 2023; Wiltschka et al. 2020, 2023). SPME is also used in a modified form in the present study.

Our study objectives were to (1) quantify the adsorption of HCB for native bentonites with different characteristics and to determine the magnitude of adsorption strength, (2) evaluate the influence of different mineral characteristics on adsorption intensity, and (3) comparatively quantify the adsorption of HCB for selected size fractionated bentonites after cation exchange (Ca^{2+}). We studied the adsorption of HCB as an HOC representative adsorptive to a set of 21 characterized bentonites as adsorbents. Since an effect of particle size and different exchangeable cations on the adsorption strength cannot be excluded for native bentonites of different origin, we performed additional adsorption experiments in which these influences were minimized. These experiments were performed with five selected bentonites after size fractionation (<2 μm) and replacement of exchangeable cations by Ca^{2+} as a cation of high environmental abundance. Furthermore, we discuss insights into relevant aspects of the use of SPME and internal standards in miniaturized adsorption experiments.

2 | Materials and Methods

2.1 | Chemicals

The HCB and $^{13}C_6$ HCB standards, respectively used as test substance and stable isotope labeled internal standard, were purchased from LGC Standards GmbH (Wesel, Germany; Dr. Ehrenstorfer Brand, 99.90 and 98.28% purity). Both were dissolved in methanol (≥99.8% purity, Ph. Eur. HPLC grade, VWR International GmbH, Darmstadt, Germany). $CaCl_2$ dihydrate (≥99%, p.a., ACS) was purchased from Carl Roth GmbH + Co. KG, Karlsruhe, Germany. Water used was of ultrapure quality (ELGA PF2XXXXM1, Veolia Water Solutions & Technologies, High Wycombe, UK), except for the deionized water from the research facility's pipeline network, which was prepared by reverse osmosis (RO-water) and used for size fractionation and cation exchange.

2.2 | Mineral Materials

Adsorption experiments were carried out with 21 smectite-rich bentonites selected from a set of 40 well-characterized bentonites (Kaufhold and Dohrmann 2008; Kaufhold et al. 2008, 2012). The selected materials included bentonites B 1, 3–7, 10, 12–14, 18, 21–23, 25–27, 29, 33, 34, and 36 (Figure 1).

Of these, the five bentonites B 5, 6, 18, 27, and 33 were selected for additional adsorption experiments based on preliminary experiments, high smectite content, and representative layer charge density (LCD). These bentonites were further prepared by size fractionation (<2 μm) and homoionic cation exchange (Ca^{2+}). The selection of 21 bentonites from the set of 40 bentonites was based on the following criteria: (1) The smectite content should be as high as possible, while at the same time ensuring that (2) no expected interfering constituents are present, (3) the number and amount of other constituents are as low as possible, and (4) the selected bentonites cover a wide range of LCD.

FIGURE 1 | Overview of the bentonite materials used. Bold numbers refer to the subset of five bentonites used in additional adsorption experiments.

Based on the available literature and preliminary experiments, quartz, feldspar, and kaolinite were addressed as minor or non-interfering constituents, while illite-containing materials were excluded (except B 25 for exemplary reason) due to relevant HCB adsorptivity (log K_d: 2.2; Böhm et al. 2023). Other accepted minor constituents included, for example, calcite, gypsum, hematite, and anatase. The mineral composition of bentonites is provided in Table 1. Overall, the selected bentonites had a smectite content of 75%–92% (84%–92% for the subset of five bentonites) and covered an LCD in a range of 0.20–0.37 eq FU^{-1} (0.21–0.36 eq FU^{-1} for the subset of five bentonites; Table 2).

2.3 | Preparation of Bentonites and Size-Fractionated Bentonites

The subset of five bentonites was finely ground using a structure-preserving cross beater mill with a sieve insert of 100-μm mesh size at the Federal Institute for Geosciences and Natural Resources (BGR, Hanover, Germany). However, the mesh size of 100 μm resulted in the rapid clogging of the sieve insert, and grinding took a very long time. To avoid clogging of the sieve insert and save time, the remaining bentonites were finely ground in a structure preserving cross beater mill with a 500-μm mesh size sieve insert at the Forschungsinstitut für Glas—Keramik GmbH (FGK), Höhr-Grenzhausen, Germany. Dry matter content of bentonites was determined at 105 and 200°C (Table S2).

In addition to grinding, the subset of five bentonites was fractionated to achieve respective subfractions of ≤2 μm particle size. Size fractionation was similar to the procedure described in Böhm et al. (2023) based on the method described by Tributh and Lagaly (1986) and Lagaly and Dékány (2013) but with further modifications. The finely ground bentonites were suspended in large 4-L glass cylinders (sedimentation cones) without pretreatment

TABLE 1 | Mineral composition of studied bentonites.

Bentonite	Smectite (%)	Kaolinite (%)	Quartz (%)	Cristobalite (%)	Feldspars (%)	Carbonates (%)	Further constituents to 100%
B1	78		3	<0.5	18	1	[a]
B3	89		1	2	7	<0.5	[a]
B4	91		2		5		[a,b]
B5	**88**		**1**		**2**	**5**	[a,c,d]
B6	**91**				**8**	**<0.5**	[a]
B7	91		2		4	2	
B10	89		6			1	[a,e,f]
B12	91		1		<0.5	1	[d,e,g]
B13	84	3	6		1	4	[a,g]
B14	88	3	3		3	1	[a]
B18	**92**		**2**		**5**	**1**	
B21	80		1	1	18		
B22	76		4	12	8	<0.5	
B23	80		10		10		
B25	61	4	13		5	<0.5	[h]
B26	86		1	8	4	1	
B27	**84**		**4**	**5**	**5**	**1**	[d]
B29	89	5	6		<0.5		
B33	**88**		**3**	**1**	**7**	**1**	[d]
B34	77	4	16		2		[a]
B36	75	2	11	3	8		[a]

Note: Data from Kaufhold et al. (2012). Bold formatted samples refer to the selected subset of five bentonites.
[a]Rutile + anatase (0%–2%).
[b]Barite (1%).
[c]Pyrite (1%).
[d]Gypsum (0%–1%).
[e]Hematite (1%).
[f]Ilmenite (1%).
[g]Fluorapathite (1%–4%).
[h]Illite (17%).

(10–20 g bentonite per cylinder). Dispersion of the materials was achieved due to the large volume of water. After a defined time of gravity settling, only the fraction of particles with a size of ≤2 μm (based on equivalent diameter) remained in the supernatant. The time required to prevent the presence of particles >2 μm in the water column of defined depth was calculated according to Stokes' law with a specific mass density of $\rho = 2.25$ g cm^{-3}. The supernatants were then siphoned off and transferred to buckets, where suspended materials were precipitated by the addition of excess $CaCl_2$. This process was repeated until the supernatant became clear (for at least 10 times and up to 25 times). The clay fraction was concentrated by removing the clear supernatants using a water aspirator pump. After full collection and concentration, additional replacement of exchangeable cations by Ca^{2+} was performed with a Ca^{2+} concentration of at least fivefold of cation exchange capacity (CEC) with a liquid:solid ratio < 4 (based on w/w%), following the recommendations of Steudel and Emmerich (2013). The concentrated samples were rinsed with RO-water to remove Cl^- ions (verification by Quantofix Chloride test strips, Macherey–Nagel). Fractions were then adjusted to an aqueous concentration of 0.01 mol $CaCl_2$ L^{-1} by repeated sequence of filling, equilibration, centrifugation, and aspiration. Finally, the suspended clays were adjusted to concentrations of 45–85 mg clay mL^{-1} in 0.01 mol $CaCl_2$ L^{-1} and stored dark and cool (4°C). Final concentrations were determined by dry matter analysis at 105°C. Prior to use in adsorption experiments, suspensions were shaken over night at room temperature and treated with ultra-sonication.

2.4 | Batch Adsorption Experiments

Adsorption experiments followed a modified procedure according to test guideline 106 of the Organisation for Economic Cooperation and Development (OECD TG 106; Organisation for Economic Cooperation and Development 2000) as described in Böhm et al. (2023), but with further optimization amended. All experiments were performed with constant mineral masses

TABLE 2 | Overview on selected bentonite characteristics of the studied bentonites.

Bentonite	LCD [a,i] (eq FU^{-1})	Tetrahedral charge [b,j] (%)	SSA [c,i] (m^2 g^{-1})	SiO_2: Al_2O_3 [k]	pH [l]	Conductivity [k] (µS)	C_{total} [d,l] (%)	TOC [e,l] (%)	TIC [f,l] (%)	CEC [g,k] (mmol 100 g^{-1})	Na^+ [k] (mmol 100 g^{-1})	K^+ [k] (mmol 100 g^{-1})	Mg^{2+} [k] (mmol 100 g^{-1})	Ca^{2+} [k] (mmol 100 g^{-1})	Σ sand [h,m] (%)	Σ silt [h,m] (%)	Σ clay [h,m] (%)
B1	0.36	11	14	3.2	8.5	161	0.2	0	0.1	97	17	2	45	52	31.2	52.4	16.4
B3	0.33	15	63	3.1	7.5	34	0	0	0	105	12	2	35	53	33.1	41.9	25.0
B4	0.31	23	46	3.2	7	127	0	0	0	108	19	2	46	38	34.3	41.8	23.9
B5	**0.31**	**19**	**65**	**3.0**	**7.3**	**306**	**0.6**	**0**	**0.6**	**100**	**14**	**3**	**33**	**67**	**30.4**	**50.2**	**19.4**
B6	**0.33**	**10**	**42**	**2.9**	**8.6**	**54**	**0**	**0**	**0**	**107**	**17**	**2**	**36**	**52**	**20.1**	**46.8**	**33.1**
B7	0.33	16	59	3.2	9.9	365	0.2	0	0.2	98	66	5	5	33	4.8	13.0	82.3
B10	0.33	37	67	3.6	9.2	219	0.1	0.1	0.1	96	28	2	22	54	2.2	16.7	81.2
B12	0.35	15	40	3.5	9.2	424	0.1	0	0.1	108	56	1	26	41	9.0	23.1	67.9
B13	0.37	63	102	2.8	8	86	0.5	0.1	0.5	84	1	2	38	75	19.7	59.8	20.5
B14	0.33	60	130	2.7	7.8	95	0.2	0.1	0.1	84	1	3	41	48	8.1	65.1	26.9
B18	**0.36**	**15**	**43**	**3.2**	**9.3**	**207**	**0.2**	**0.1**	**0.1**	**105**	**28**	**3**	**37**	**46**	**15.5**	**50.4**	**34.1**
B21	0.34	28	23	2.6	7.9	266	0	0	0	91	42	3	29	30	28.5	43.6	27.9
B22	0.35	7	31	4.2	8.8	145	0	0	0	93	66	1	3	27	0.8	34.2	64.9
B23	0.36	9	7	3.4	9	95	0	0	0	101	68	1	2	33	5.5	26.6	68.0
B25	0.30	30		3.0	7.4	17	0.1	0.1	0	63	0	2	15	41	13.3	67.0	19.7
B26	0.35	18		4.5	9.5	158	0.2	0.1	0.1	93	20	3	16	49	6.1	42.9	50.9
B27	**0.21**	**8**	**32**	**3.1**	**9.7**	**382**	**0.9**	**0.1**	**0.9**	**92**	**62**	**2**	**5**	**31**	**3.9**	**12.7**	**83.5**
B29	0.33	31	96	2.4	6.4	15	0.1	0.1	0	76	0	1	23	44	50.6	43.1	6.3
B33	**0.25**	**12**	**16**	**3.0**	**9.4**	**342**	**0.1**	**0.1**	**0.1**	**82**	**57**	**2**	**5**	**33**	**2.5**	**16.5**	**81.1**
B34	0.37	36	24	3.7	7.7	124	0.1	0.1	0	85	5	1	29	55	29.0	50.7	20.3
B36	0.20	51	57	3.5	7.1	35	0.1	0.1	0	56	0	2	17	36	42.3	47.7	10.0

Note: Bold formatted samples refer to the selected subset of five bentonites.
[a]Layer charge density (alkylammonium method; equivalent charge per formula unit).
[b]Portion of tetrahedral charge to total charge.
[c]Specific surface area (BET-N_2 physisorption, except for B27 as BET-Ar).
[d]Total carbon.
[e]Total organic carbon.
[f]Total inorganic carbon.
[g]Cation exchange capacity.
[h]From particle size distribution analysis (sand: 2000–63 µm; silt 63–2 µm; clay < 2 µm).
[i]Kaufhold et al. (2010).
[j]Kaufhold et al. (2017).
[k]Kaufhold and Dohrmann (2008).
[l]Kaufhold et al. (2008).
[m]This study.

suspended in a 0.01 mol $CaCl_2$ L^{-1} solution and spiked with varying HCB concentrations. Each adsorption experiment yielded one adsorption isotherm from which a solid–liquid distribution coefficient, K_d, was derived. The isotherms were determined with five different HCB concentrations (1, 2, 3, 4, 5 µg L^{-1}) within the water solubility range of HCB (Table S1). The procedure varied slightly depending on bentonite selection (subset of five vs. further bentonites) and particle size of bentonites (<100/500 µm vs. <2 µm): With regard to replications, multiple experiments were performed for the subset of five bentonites to achieve at least four isotherms per bentonite. For the further 16 bentonites, single isotherms without replicates were determined due to time constraints and sufficient validity of the results.

For experiments with the bentonites <100/500 µm, a specific bentonite mass of 150 ± 1.5 mg was weighed in multiples to 20-mL glass vials (CS Chromatographie Service, Langerwehe, Germany). The adsorbents were then suspended in 15 mL aqueous solution containing 0.01 mol $CaCl_2$ L^{-1} and shaken for 24 h to ensure sufficient swelling and equilibrium conditions of adsorbents and solution. For the subset of five bentonites, additional adsorption experiments were performed with specifically increased or rather decreased masses of bentonite to assure that resulting adsorption is independent of the sorbent mass. These experiments were performed with 75–250 mg bentonite per glass vial. Specific bentonite concentrations are provided together with the results.

For experiments with bentonites <2 µm, suspension aliquots (1.45–3.85 mL) containing a defined bentonite mass were transferred by Eppendorff pipette to the 20-mL headspace vials and diluted with 0.01 mol L^{-1} $CaCl_2$ solution to a total volume of 12.8 mL per vial (the smaller volume allowed saving of bentonite material).

The bentonite suspensions with different HCB concentrations were equilibrated for 24 h on a horizontal shaker at 200 rpm (Innova 2300 platform shaker; New Brunswick Scientific). Preliminary tests on adsorption kinetics resulted in an equilibration time of $t_{95\%}$ < 2 h at 200 rpm for all bentonites of the subset of five (<100 µm). However, due to decreased deviation of adsorption coefficients within 20 h and beneficial laboratory handling, equilibration was set to 24 h for all experiments (Figure 2).

After equilibration, samples were centrifuged for 30 min at 939 RCF (2000 rpm; Hettich Rotanta 460 R centrifuge). Full separation of fine particles was visually assured by a completely clear supernatant. Afterward, 10 mL aliquots of supernatants were transferred to fresh brown glass vials with magnetic caps (CS Chromatographie Service). Subsequently, ^{13}C labeled HCB was added as the internal standard for HCB analysis. Vials were closed and then analyzed for analyte and internal standard by SPME coupled to gas chromatography-mass spectrometry (GC-MS).

2.5 | Extraction and Analysis (SPME-GC-MS)

Samples from adsorption experiments were measured in sequences with a 10-point external calibration (0.02–5 µg HCB L^{-1}, including ^{13}C HCB) and blank samples (both pure $CaCl_2$ solution and bentonite suspension without HCB) for quality control. General details on SPME and on laboratory specific adjustments were given in own previous studies (Böhm, Schlechtriem, and Düring 2016; Böhm et al. 2017, 2023; Wiltschka et al. 2020, 2023). Briefly, samples were extracted by headspace (HS)-SPME using fibers with a 100 µm polydimethylsiloxane (PDMS) coating (Supelco/Sigma-Aldrich brand, Merck, Darmstadt, Germany). Extraction was performed for 30 min at 50°C and 500 rpm in the agitator (combined heating/shaking device). Samples were pre-equilibrated in the agitator for 11 min. After extraction, HCB was thermally desorbed from the fiber in the injection system of the GC-MS for 3 min at 240°C. Quality assurance and quality control for SPME extraction included pre-heating of the fiber before extraction, measuring of blank samples, usage of fresh glass vials, as well as visual fiber control and, if necessary, cleaning of the fiber with methanol (Böhm et al. 2023). Detailed parameters on instrumentation and GC-MS conditions are given in Table S3 and subsequent text in the Supporting Information.

2.6 | Calculation of Adsorption

Adsorption isotherms were calculated according to OECD TG 106 (Organisation for Economic Cooperation and Development 2000) based on freely dissolved or rather aqueous HCB concentrations (C_{aq}) and adsorbed HCB concentrations (C_s). The respective quotients C_s/C_{aq} for the initially spiked HCB concentrations result in a sequence of points from which a linear regression is obtained in case of proportionally increasing adsorption with increasing initial HCB concentration. The linear regression corresponds to the linear (Henry type) adsorption isotherm, and the distribution coefficient K_d is derived from the slope of the isotherm. Isotherms were plotted as regressions through the origin (Chappell et al. 2020). The aqueous HCB concentrations (C_{aq}) in aliquots from the adsorption experiments were calculated based on internal standard corrected peak areas of both adsorption samples and external calibration. Adsorbed concentrations C_s were calculated following OECD TG 106 (Organisation for Economic Cooperation and Development 2000) according to Equation (1) as similarly summarized in Böhm et al. (2023).

$$C_s = \frac{(C_0 - C_{aq}) \times V_0}{m_B} \quad (1)$$

C_s is the concentration of HCB adsorbed to the bentonite phase at adsorption equilibrium (µg g^{-1}), C_0 is the initial HCB concentration of the aqueous solution in contact with the bentonite phase (µg mL^{-1}), C_{aq} is the mass concentration of HCB in the aqueous phase at adsorption equilibrium (µg mL^{-1}), V_0 is the initial volume of the aqueous phase in contact with the bentonite (mL), and m_B is the mass of the bentonite phase (g). Unless otherwise stated, all presented adsorption data are based on bentonite masses m_B that were corrected by dry matter content of materials determined at 105°C. Because smectite is expected to be the relevant adsorbent phase in the selected bentonites, the K_d values were additionally calculated after normalization to the smectite content of bentonites (Table 1).

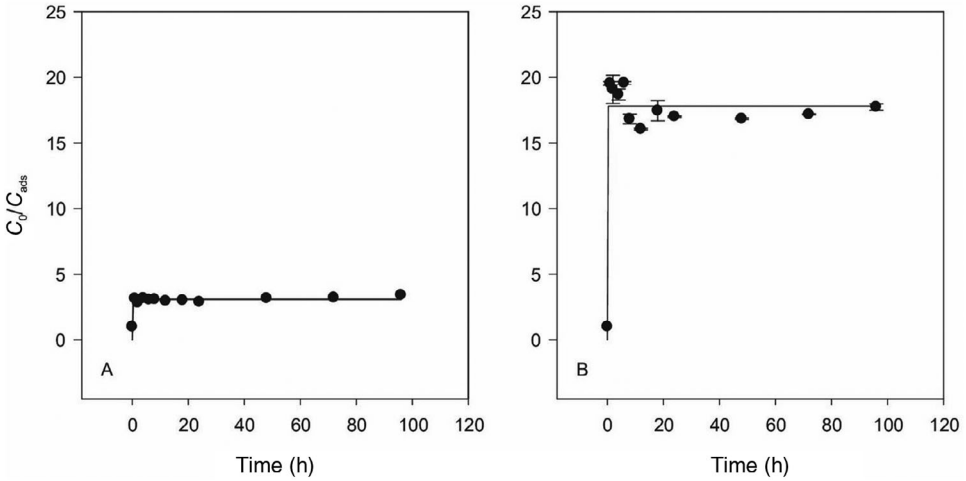

FIGURE 2 | Adsorption kinetics (time to equilibrium) of HCB exemplarily shown for the two bentonites B 5 (A) and B 27 (B). Points show adsorption by quotients of C_0 (freely dissolved HCB concentration in a system without sorbent) divided by C_{ads} (freely dissolved HCB concentration in a system including sorbent).

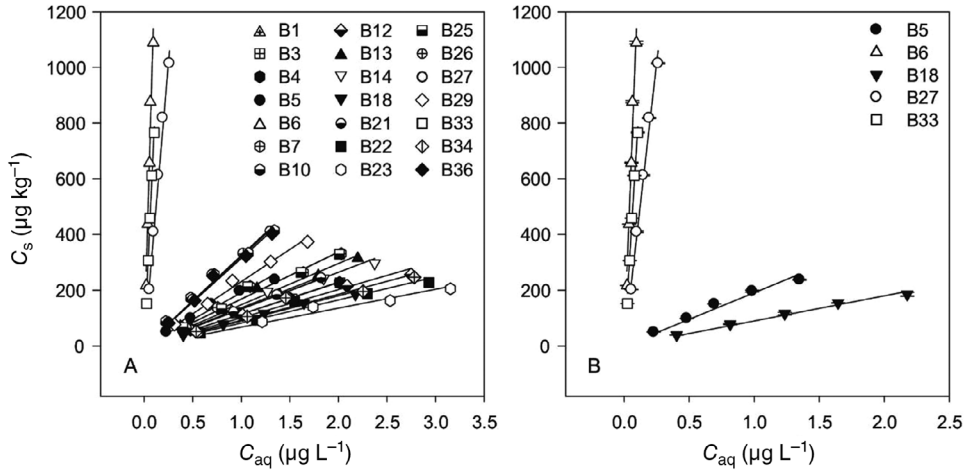

FIGURE 3 | Adsorption isotherms for the interaction of HCB with selected bentonites. (A) Overview on adsorption for all 21 tested bentonites. (B) Adsorption for the subgroup of five selected bentonites. HCB concentration: 1–5 µg L^{-1} except B1, B3, B4, and B21 with 1–4 µg L^{-1}; particle size fraction: <100 µm for the subset of five and <500 µm for the further 16 bentonites; $n = 2$ for the group of five and $n = 1$ for the further 16 bentonites; bentonite concentration: 10 g L^{-1}, except B5 and B18 with 16.7 g L^{-1}, B6 and B27 with 5 g L^{-1}, and B33 with 6.7 g L^{-1}. Although included in Figure 3A, isotherms for the subgroup of five bentonites are separately shown in Figure 3B for better differentiation and with error bars (± standard deviation, sd).

3 | Results

3.1 | HCB Adsorption to Native Bentonites

Adsorption studies with HCB and the set of selected 21 bentonites yielded adsorption coefficients K_d that varied over several orders of magnitude (K_d: ≈70–12,000; log K_d: 1.8–4.1; Figure 3, Table 3; Figure S1). Normalization of adsorption to the smectite content slightly increased adsorption coefficients (≈85–14,000; log K_d: 1.9–4.1; Table 3). Compared to a set of reference smectites (log K_d: 0.9–2.8; Böhm et al. 2023), HCB adsorption to the here used bentonites was generally higher. With a median K_d of 148 and log K_d of 2.2 (176 and 2.3 after smectite correction), HCB adsorption to bentonites was relevant in an environmental range of moderate adsorption. However, three bentonites were identified that showed unexpectedly high adsorption in a range of K_d ≈4500–12,000 (log K_d: 3.7–4.1) and in a range of K_d ≈5500–14,000 (log K_d: 3.7–4.1) after smectite correction, which is in the same order of magnitude as HCB adsorption to pure organic matter (Aldrich humic acid, K_d: 29,000; log K_d: 4.5; Böhm, Schlechtriem, and Düring 2016).

The extensive characterization of the bentonites (Kaufhold and Dohrmann 2008; Kaufhold et al. 2008, 2010, 2012) allowed the analysis of relationships between adsorption strength and a variety of mineral parameters. However, neither single nor multiple linear regression analysis could unambiguously explain a relationship between adsorption strength and bentonite properties, or rather further characterizing parameters such as mineral constituents, chemical composition, particle size, specific surface area, total, inorganic, and organic carbon content (TC, TIC, and TOC), pH, electric conductivity, cation exchange capacity, or LCD

TABLE 3 | Adsorption of HCB (1–5 μg L^{-1}) in the presence of native bentonite materials (10 g L^{-1}).

Bentonite	*N*	$K_d \pm$ sd	log $K_d \pm$ sd	$K_d \pm$ sd (SmC)	log $K_d \pm$ sd (SmC)	R^2	RMSE (*n*) [a]
B 1 [b]	1	137	2.14	176	2.24	0.9986	6.3 (4)
B 3 [b]	1	114	2.06	128	2.11	0.9985	6.0 (4)
B 4 [b]	1	115	2.06	126	2.10	0.9997	2.8 (4)
B 5	**4** [c]	**196 ± 8**	**2.29 ± 0.02**	**223 ± 9**	**2.35 ± 0.02**	**0.9897**	**20.2 (5)**
B 6	**4** [d]	**12,369 ± 518**	**4.09 ± 0.02**	**13,592 ± 569**	**4.13 ± 0.02**	**0.9825**	**59.0 (5)**
B 7	1	169	2.23	185	2.27	0.9947	16.2 (5)
B 10	1	321	2.51	360	2.56	0.9957	18.3 (5)
B 12	1	101	2.01	111	2.05	0.9916	16.3 (5)
B 13	1	148	2.17	176	2.25	0.9910	20.1 (5)
B 14	1	132	2.12	150	2.18	0.9945	15.1 (5)
B 18	**4** [c]	**106 ± 18**	**2.02 ± 0.07**	**115 ± 20**	**2.05 ± 0.07**	**0.9912**	**14.2 (5)**
B 21 [b]	1	133	2.12	166	2.22	0.9998	2.1 (4)
B 22	1	83	1.92	109	2.04	0.9895	16.1 (5)
B 23	1	68	1.83	85	1.93	0.9918	12.7 (5)
B 25	1	169	2.23	276	2.44	0.9948	15.9 (5)
B 26	1	325	2.51	378	2.58	0.9977	13.1 (5)
B 27	**7** [d]	**4547 ± 533**	**3.65 ± 0.05**	**5413 ± 634**	**3.73 ± 0.05**	**0.9947**	**28.9 (5)**
B 29	1	231	2.36	260	2.41	0.9974	12.7 (5)
B 33	**4** [e]	**8016 ± 531**	**3.90 ± 0.03**	**9109 ± 603**	**3.96 ± 0.03**	**0.9984**	**16.0 (5)**
B 34	1	93	1.97	121	2.08	0.9878	18.6 (5)
B 36	1	314	2.50	419	2.62	0.9974	13.6 (5)

Note: Solid–Liquid distribution coefficients K_d are provided for the entire material as well as normalized for the smectite content of the bentonites (SmC). *N* is the number of experiments performed, R^2 is given as measure of isotherm linearity. Bold formatted samples refer to the selected subset of five bentonites.

[a]Root-mean-square error of C_s/C_{aq} regression (*n*: number of test substance concentrations per isotherm.

[b]Experiment with 1–4 μg HCB L^{-1}.

[c]Thereof two experiments with 16.7 g sorbent L^{-1}.

[d]Thereof two experiments with 5 g sorbent L^{-1}.

[e]Thereof two experiments with 6.7 g sorbent L^{-1}.

(Tables 1–3). Results on the linear correlation between K_d and selected mineral properties (full dataset and moderate adsorptive bentonites only) are provided in Figures S2 and S3.

Forward and backward multiple regression with K_d values corrected for their smectite content suggested that K_d can be predicted from a linear relation with LCD as the independent variable only. The best linear correlations between smectite-corrected K_d values and bentonite parameters were found for LCD, LCD (fixed anions), and CEC (R^2 = 0.22–0.37; Figure 4; Figure S4).

Pearson and Spearman correlation were both performed for the whole set of 21 bentonites as well as for a subset in which the three highly adsorptive bentonites were excluded. Correlations were also calculated after correcting the adsorption data for the smectite content of the bentonites. In case of significant correlations ($\alpha < 0.05$), most often a moderate correlation with LCD and fixed anions was detected. Furthermore, correlations with the portion of tetrahedral charge, specific surface area, CEC, Na^+, and MgO were partly suggested (correlation coefficients up to 0.6; Figures S5–S8). Samples with distinct colors (Figure 1) did not stand out regarding adsorption strength, and no correlations were detected between Fe and adsorption (Figure S5–S8). Most of the bentonites do not contain any ferrous iron, and those few that do, showed no specific interactions. The redox state of the samples was determined before, both by Mössbauer spectroscopy and titration (Chiou et al., 2021), but no impact on adsorption strength was found as well. Redox state and (ferrous) Fe content of samples were therefore not further considered.

3.2 | HCB Adsorption to Size Fractionated Ca-Modified Bentonites

HCB adsorption to size fractionated and Ca-modified bentonites resulted in K_d values of ≈75–6000 (log K_d: 1.9–3.8; Table S4). Adsorption to these bentonite fractions is reduced compared to the respective five native bentonites of particle size <100 μm (log K_d: 2.0–4.1; Figure 5; Table S4).

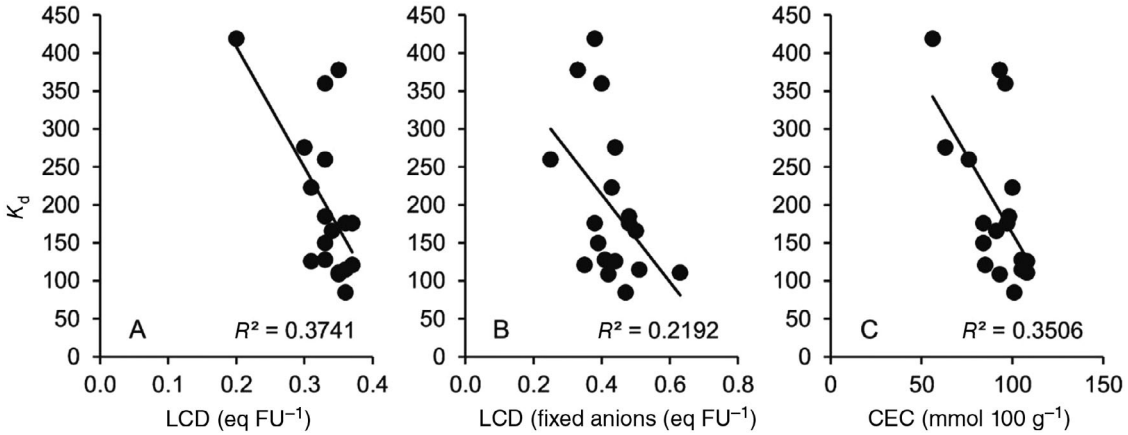

FIGURE 4 | Relationships between K_d values corrected for smectite content and the mineral properties (A) Layer charge density (LCD), (B) LCD (fixed anions), and (C) cation exchange capacity (CEC). Plotting for 18 smectite-corrected bentonites (full dataset of 21 bentonites excluding the three highly adsorptive bentonites B6, B27, and B33). Trend lines and R^2 refer to linear correlation.

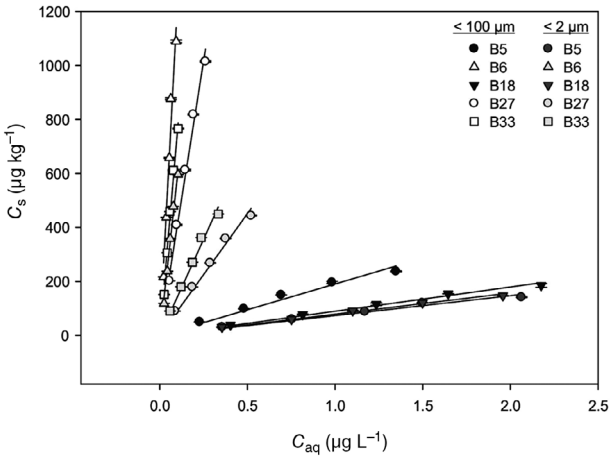

FIGURE 5 | HCB adsorption to size fractionated and Ca-modified bentonites (<2 µm) and comparison with adsorption to the five respective native bentonites (<100 µm). HCB concentration: 1–5 µg L^{-1}; number of experiments per bentonite type: $N = 2$; bentonite concentrations (<100 µm): B5 and B18 with 17 g L^{-1}, B6 and B27 with 5 g L^{-1}, and B33 with 7 g L^{-1}; bentonite concentrations (<2 µm): B5 and B18 with 21 g L^{-1}, B6 with 8 g L^{-1}, and B27 and B33 with 10 g L^{-1}), error bars: ± standard deviation (sd).

4 | Discussion

4.1 | Considerations on Methodology and Experimental Design

Miniaturized batch adsorption experiments combined with SPME coupled to GC–MS for extraction and analysis provided sorption data with excellent reproducibility, with reduced laboratory work, without toxic solvents, and with a lower demand of sorbent material compared to "classic" approaches. The latter is particularly relevant for size-fractionated and cation-modified sorbents, of which often only small amounts can be prepared with reasonable effort. At the same time, this highlights a demand for experimental and analytical precision that ensures sufficiently low variation to be able to confidently differentiate between results. Correction of analytical raw data with a stable isotope-labeled internal standards (Böhm et al. 2017; Bondarenko and Gan 2009; Poerschmann et al. 1997; Wiltschka et al. 2020, 2023), as used in this study, is considered best practice for SPME measurements that allow the analysis of trace concentrations from miniaturized batch adsorption experiments. However, the use of stable isotope-labeled internal standards is not generally applicable in adsorption experiments. In addition to commercial and financial requirements (availability of standards, available budget), an important prerequisite for the use of internal standards is that no (relevant proportion of the) sorbent remains in the solution to be measured. Therefore, the internal standard was added after test substance equilibration, sample centrifugation, and aliquoting of the supernatant. In case of a substantial amount of remaining adsorbent, the internal standard would adsorb in the sample to be measured. This would affect the extracted amount of internal standard, thereby the internal standard correction, and consequently the calculation of test substance concentration. With regard to the multiphase system that a batch adsorption experiment represents, applicability is therefore given only if suspended sorbents can be separated, for example, by centrifugation, to allow aliquoting of the sorbent-free supernatant for measurement of the equilibrium C_{aq} of the test substance. Unlike dissolved or lower density organic matter and dispersed clay particles, this requirement is easily met for larger particles (e.g., silt) and coagulated clay particles.

In this study, special emphasis was placed on ensuring linear adsorption isotherms, which can be achieved by changing the sorbent mass or rather the sorptive concentration in the test system. For (highly) hydrophobic substances with a very low water solubility, a strong reduction of the sorptive concentration is not desirable to assure reliability and validity of trace analysis. Thereby, the water solubility range of the test substance largely determines its possible concentration range in the adsorption experiment. Consequently, the adjustment of adsorbent masses is the relevant influencing factor to ensure both valid analysis and isotherm linearity, that is, assuring that the sorbent concentration is neither too high (then analysis of the substance could be prevented by an insufficient limit of quantification of the method/analytical instrument) nor too low (then the reduction in

substance concentration could not be reliably differentiated from the spiked concentration considering the analytical variation, or the adsorption isotherm might level off). This could be challenged with regard to environmental relevance, especially when chemicals occur in high environmental concentrations or when the adsorption capacity of a material is of interest. However, for HOCs like HCB, with freely dissolved environmental concentrations in the range of pg–µg L^{-1}, a proportional increase in adsorption with increasing aqueous analyte concentrations can be expected to be environmentally relevant due to a surplus of sorption sites on extensively available sorbent material. Linear isotherms are then not only justified in terms of environmental relevance but are also advantageous because they allow a proportional comparison between orders of magnitude as well as a straightforward calculation of HOC retention coefficients for transport considerations. The comparison of adsorption strength using K_d´s derived from linear sorption isotherms is especially useful for analyzing the adsorption of different adsorbent-chemical combinations based on interaction experiments with both HOCs of widely varying hydrophobicity/water solubility and adsorbents of widely varying adsorptivity.

4.2 | HCB Adsorption to Native Bentonites

Owing to the generally much higher share of mineral constituents compared to organic matter in arable soils (mostly below 5% soil organic carbon; Drexler et al. 2022; Gerzabek et al. 2005), an environmental relevance of HOC sorption to CM is already given for the majority of bentonites with moderate HCB adsorptivity. However, the environmental relevance of HCB adsorption is expected to be very high for the highly adsorptive bentonites, where high adsorptivity and high environmental occurrence add up. This can be the case in regions where such highly adsorptive bentonites occur or in technical bentonite applications, such as linings of polluted sites or landfills, or treatment of polluted waters. Here, the differences between clay minerals of geogenic and pedogenic origin have to be considered. To our best knowledge, our results show for the first time that native bentonites can exhibit such high adsorptivity for HOCs, that is, in the same range as pure OM phases. With regard to process-oriented explanations, especially the causality of a relationship between adsorption strength and varying permanent layer charge would have been reasonable (i.e., increasing adsorption of neutral, hydrophobic compounds with decreasing layer charge). However, LCD could not be verified to be the decisive parameter by linear correlation of the experimental data (correlation of K_d [and smectite-corrected K_d] (Table 3, columns 3 and 5) and LCD (Table 2, column 2), $R^2 = 0.11$ [0.12] or rather $R^2 = 0.27$ [0.37] with the highly adsorptive bentonites excluded; Figures S2–S4). The correction for the smectite content improves the correlation between adsorption and mineral parameters, but the R^2 remains <0.4 for all linear correlations. Supposed correlations with Pearson and Spearman correlation coefficients of up to 0.6 for selected mineral properties are regarded reliable based on further consideration of data. However, after plotting of data for K_d and respective mineral parameters, the uncertainty of reliable relationships is visualized. Exemplarily, coherence of the relationship between K_d and LCD is dependent on the three bentonites B10, B26, and B36 with $K_d \approx 320$ [range after correction for smectite content: 360–420] (Figure 4A; Figures S3 and S4). Selective exclusion of data for either B10 and B26 or rather B36 would change the R^2 to either 0.66 [0.71] or rather 0.08 [0.11]. Also, quantum chemical calculations of HCB interactions with Ca-montmorillonite showed no evident relationship between adsorption and LCD (001 models, where the layer charge was systematically varied by varying Al/Mg substitutions in the octahedral sheet; Grančič et al. 2023): Calculations revealed the existence of multiple geometric optima with different interaction energies. In these systems, the variation of interaction energy depending on geometric optima far exceeded potential influences of varying layer charge.

Hu et al. (2019) identified the SiO_2:Al_2O_3 ratio and LCD to be particularly relevant for adsorption to zeolites. However, in the present study, the intensity of HCB adsorption to the set of bentonites could not be explained by these parameters. The lack of recognizable correlations may be influenced by multiple parameters of mineral characteristics, none of which dominate over the others. Excluding the highly adsorptive bentonites (B6, B27, B33; Table 3, Figure 3), K_d values vary by a factor of ≈5. However, these values are all in a similar range of adsorption and none of the mutually influencing mineral characteristics is a dominant driver for the moderate differences in adsorption. Contrary, the three further bentonites B6, B27, and B33 provide larger adsorption by 1–2 orders of magnitude. Here, we expect that a major parameter is clearly deviating and thereby identifiable. According to this logic, the causal parameter(s) is(are) not yet known. A similarity based on the formation of the bentonites can be ruled out due to the different origin of these highly adsorptive bentonites (Wyoming and Milos). Samples B27 and B33 are both from the famous Wyoming bentonite mining district, and both performed similarly. Bentonite B6 from Milos showed as high HCB adsorption capacity as the Wyoming bentonites but much more than the other bentonites from Milos (B3, B4, B5, and B7). The fact that the two Wyoming bentonites and only one sample from Milos showed exceptionally high HCB adsorption may allow to exclude an effect of individual parameters for the highly adsorptive bentonites. The type of exchangeable cation (Ca/Mg–Na) does not play a significant role, which is in agreement with cation modified adsorption experiments for these specific cations (Böhm et al. 2023). Also, particle or aggregate size cannot explain the significant differences of the three bentonites compared to the others. With respect to the adsorption of HCB on surfaces, the possible importance of the hydrophobicity of the respective surface was discussed. In case of smectites, one would expect higher hydrophobicity in case of low charge density (as typical of Wyoming bentonites) because of the presence of less exchangeable cations per interlayer area which in turn represent the hydrophilic sites. This could explain the performance of the Wyoming bentonites but not that of B6, which has an intermediate LCD. In addition, the low charged material B36 did not show high adsorption capacity. Wyoming bentonites are known for the low specific surface area which results from comparably well-preserved quasi crystals (Kaufhold et al. 2010). The intermediate specific surface area of B6, however, does not allow to conclude an effect of the specific surface area. Wyoming bentonites are also known to contain some reactive silica (a form of opal), which could provide some hydrophobic adsorption sites but sample B6 does not contain reactive silica, which in turn can also be excluded. Overall, no parameter could be identified which would indicate a compositional difference of

B6 compared with the other Milos bentonites and at the same time a similarity with the Wyoming bentonites. This suggests either that a combination of different parameters promotes the HCB adsorption or that the characterization of the bentonites performed so far has not been sufficient to identify the most relevant parameter determining the adsorption. Based on pore distributions derived from specific surface area measurements, there is evidence for an influence of microporosity on adsorption, which is consistent with considerations from previous works (Cheng, Hu, and Hu 2012; Hu et al. 2019). However, further experimental consideration of pore size distributions will be subject of our following studies.

4.3 | HCB Adsorption to Size Fractionated Ca-Modified Bentonites

With the K_d values of Ca^{2+}-modified bentonite fractions <2 μm accounting for ~20%–75% of the native bentonites (Table S4), the relevance of cation configuration and particle size is highlighted. Generally, reduced particle size is expected to increase adsorption due to increased specific surface area, which is in line with an observed general trend of increasing adsorption with increasing surface area and/or porosity in most chemically and physically variable material classes (e.g., Mayer 1994; Pérez-Botella, Valencia, and Rey 2022; Strauss, Brümmer, and Barrow 1997; Zhang et al. 2022). This is opposite in the present study and differs from the size fractionated and Ca^{2+} treated smectite in Böhm et al. (2023), where the K_d slightly increased after Ca^{2+} treatment. A qualitative shift in the share of mineral constituents has to be assumed (exemplarily, quartz, feldspar, and clay minerals have different particle size ranges in which they usually occur). This should largely lead to increased adsorption due to the decreased relative share of especially quartz but also of feldspar (negligible adsorption for both), while the relative share of smectites is increased (relevant adsorption). Therefore, it can be assumed that the Ca^{2+} modification was the main driver for the reduced HCB adsorption to the bentonite fractions <2 μm. This is in line with HCB adsorption to a reference smectite after cation modification with different alkaline earth and alkali cations in our previous study. There, the lowest adsorption was observed after alkaline earth cation modification, which was attributed to greater charge density and cation hydration of alkaline earth cations leading to decreased stability of HCB–cation interactions and potentially decreased surface hydrophobicity (Böhm et al. 2023).

5 | Conclusions

The miniaturized batch adsorption method used reduces the amount of sorbents and toxic chemicals required, while providing excellent sensitivity and reproducibility. Its use is especially recommended both for test substances with low water solubility and when only small amounts of sorbent material are available. HOC adsorption to native, smectite-rich bentonites is mostly moderate (log K_d = 1.8–2.5) but can be as high as adsorption to pure organic matter phases (here up to log K_d = 4.1). Normalization of adsorption to the smectite content of bentonites mostly enhanced the strength of correlation between adsorption and mineral parameters, but was not the solution to full explanation of interactions. For the moderately adsorptive bentonites, the variation of adsorption might be influenced by a combination of multiple parameters. After correction for smectite content, adsorption was best explained by LCD and CEC with an R^2 of 0.37/0.35. However, from more than 20 characterizing parameters, no single or multiple correlation could be identified for the comprehensive explanation and prediction of adsorption. Hence, a set of ≈20 bentonites may not be sufficient for an unambiguous elucidation of parameters for the prediction of adsorption strength based on mineral properties. This prediction is further complicated by the mutual influence of the individual parameters, which may include additional parameters not previously considered, especially for the bentonites with strongest adsorption of HCB. When comparing HCB adsorption to the subset of five native bentonites (log K_d: 2.0–4.1) with respective size-fractionated and cation-modified bentonites (1.9–3.8), an adsorption-reducing influence of Ca^{2+} is expected to exceed an adsorption-increasing effect of reduced particle size and higher proportion of smectites. The findings of our study contribute to the further elucidation of HOC–CM interactions. Knowledge of bentonite materials with high adsorptivity for hydrophobic organic compounds can further provide valuable advantages for the selection of materials for research and development approaches, for example, for the use of bentonite in landfill sealings or for the enhancement of super adsorbents for water treatment.

Acknowledgments

We acknowledge support by Deutsche Forschungsgemeinschaft (DFG) and Fonds zur Förderung der Wissenschaftlichen Forschung (FWF) in the bilateral project "Clay minerals as sorbents for hydrophobic organic chemicals—ClayHOC" (DFG: BO5388/1–1, 443637168; FWF: I 4876-N). Leonard Böhm acknowledges additional funding from a fund of the Justus Liebig University Giessen to support postdocs and tenure-track faculty with family responsibilities. We further acknowledge the assistance of Mona Trabold in the sedimentation fractionation of the bentonites.

Open access funding enabled and organized by Projekt DEAL.

Data Availability Statement

The data that support the findings of this study are provided in the article and the Supporting Information. Further data are available from the corresponding author upon reasonable request.

References

Ahmed, A. A., S. Thiele-Bruhn, S. G. Aziz, et al. 2015. "Interaction of polar and nonpolar organic pollutants with soil organic matter: Sorption experiments and molecular dynamics simulation." *Science of the Total Environment* 508, no. 1: 276–287. https://doi.org/10.1016/j.scitotenv.2014.11.087.

Arthur, C. L., and J. Pawliszyn. 1990. "Solid Phase Microextraction With Thermal Desorption Using Fused Silica Optical Fibers." *Analytical Chemistry* 62, no. 19: 2145–2148. https://doi.org/10.1021/ac00218a019.

Awad, A. M., S. M. Shaikh, R. Jalab, et al. 2019. "Adsorption of Organic Pollutants by Natural and Modified Clays: A Comprehensive Review." *Separation and Purification Technology* 228: 115719. https://doi.org/10.1016/j.seppur.2019.115719.

Bailey, R. E. 2001. "Global Hexachlorobenzene Emissions." *Chemosphere* 43, no. 2: 167–182. https://doi.org/10.1016/S0045-6535(00)00186-7.

Barber, J. L., A. J. Sweetman, D. Van Wijk, and K. C. Jones. 2005. "Hexachlorobenzene in the Global Environment: Emissions, Levels,

Distribution, Trends and Processes." *Science of the Total Environment* 349, no. 1–3: 1–44. https://doi.org/10.1016/j.scitotenv.2005.03.014.

Böhm, L., R. A. Düring, H. J. Bruckert, and C. Schlechtriem. 2017. "Can Solid-Phase Microextraction Replace Solvent Extraction for Water Analysis in Fish Bioconcentration Studies With Highly Hydrophobic Organic Chemicals?" *Environmental Toxicology and Chemistry* 36, no. 11: 2887–2894. https://doi.org/10.1002/etc.3854.

Böhm, L., P. Grančič, E. Scholtzová, et al. 2023. "Adsorption of the Hydrophobic Organic Pollutant Hexachlorobenzene to Phyllosilicate Minerals." *Environmental Science and Pollution Research* 30, no. 13: 36824–36837. https://doi.org/10.1007/s11356-022-24818-4.

Böhm, L., C. Schlechtriem, and R. A. Düring. 2016. "Sorption of Highly Hydrophobic Organic Chemicals to Organic Matter Relevant for Fish Bioconcentration Studies." *Environmental Science & Technology* 50, no. 15: 8316–8323. https://doi.org/10.1021/acs.est.6b01778.

Bondarenko, S., and J. Gan. 2009. "Simultaneous Measurement of Free and Total Concentrations of Hydrophobic Compounds." *Environmental Science & Technology* 43, no. 10: 3772–3777. https://doi.org/10.1021/es8037033.

Chappell, M. A., J. M. Seiter, H. M. West, et al. 2020. "Organic Contaminant Sorption Parameters Should Only Be Compared Across a Consistent System of Linear Functions." *Heliyon* 6, no. 3: e03511. https://doi.org/10.1016/j.heliyon.2020.e03511.

Cheng, H., E. Hu, and Y. Hu. 2012. "Impact of Mineral Micropores on Transport and Fate of Organic Contaminants: A Review." *Journal of Contaminant Hydrology* 129: 80–90. https://doi.org/10.1016/j.jconhyd.2011.09.008.

Chiou, W.-A., R. Dohrmann, S. Kaufhold, M. Plötze, J. W. Stucki, and K. Ufer. 2021. "Sample characterization." In *Bentonites: Characterization, Geology, Mineralogy, Analysis, Mining, Processing and Uses*, edited by S. Kaufhold, 1–314. E. Schweizerbart Science Publishers. https://doi.org/10.1127/bentonites/9783510968596.

Desforges, J.-P., A. Hall, B. McConnell, et al. 2018. "Predicting Global Killer Whale Population Collapse From PCB Pollution." *Science* 361, no. 6409: 1373–1376. https://doi.org/10.1126/science.aat1953.

Drexler, S., G. Broll, H. Flessa, and A. Don. 2022. "Benchmarking Soil Organic Carbon to Support Agricultural Carbon Management: A German Case Study." *Journal of Plant Nutrition and Soil Science* 185, no. 3: 427–440. https://doi.org/10.1002/jpln.202200007.

Georgieva, I., D. Tunega, A. J. Aquino, and H. Lischka. 2023. "A Theoretical Adsorption Study of the Inner-Core and Outer-Core Hydrated Alkali Metal Cation–Circumcoronene Complexes." *International Journal of Quantum Chemistry* 123, no. 24: e27100. https://doi.org/10.1002/qua.27100.

Gerzabek, M. H., F. Strebl, M. Tulipan, and S. Schwarz. 2005. "Quantification of Organic Carbon Pools for Austria's Agricultural Soils Using a Soil Information System." *Canadian Journal of Soil Science* 85: 491–498. https://doi.org/10.4141/S04-083.

Grančič, P., L. Böhm, M. H. Gerzabek, and D. Tunega. 2023. "On the Nature of Hydrophobic Organic Compound Adsorption to Smectite Minerals Using the Example of Hexachlorobenzene-Montmorillonite Interactions." *Minerals* 13, no. 2: 280. https://doi.org/10.3390/min13020280.

Heringa, M. B., and J. L. M. Hermens. 2003. "Measurement of Free Concentrations Using Negligible Depletion-Solid Phase Microextraction (nd-SPME)." *TrAC Trends in Analytical Chemistry* 22, no. 9: 575–587. https://doi.org/10.1016/S0165-9936(03)01006–9.

Hites, R. A., T. F. Bidleman, and M. Venier. 2022. "Atmospheric Concentrations of Hexachlorobenzene and Octachlorostyrene Are Uniform Across the Great Lakes Region and Have Not Changed Much in 25 Years." *Environmental Science & Technology Letters* 9, no. 8: 660–665. https://doi.org/10.1021/acs.estlett.2c00444.

Hu, E., X. Zhao, S. Pan, Z. Ye, and F. He. 2019. "Sorption of Non-Ionic Aromatic Organics to Mineral Micropores: Interactive Effect of Cation Hydration and Mineral Charge Density." *Environmental Science & Technology* 53, no. 6: 3067–3077. https://doi.org/10.1021/acs.est.9b00145.

Jaynes, W. F., and S. A. Boyd. 1991. "Hydrophobicity of Siloxane Surfaces in Smectites as Revealed by Aromatic Hydrocarbon Adsorption From Water." *Clays and Clay Minerals* 39, no. 4: 428–436. https://doi.org/10.1346/CCMN.1991.0390412.

Kaufhold, S., and R. Dohrmann. 2008. "Detachment of Colloidal Particles From Bentonites in Water." *Applied Clay Science* 39, no. 1–2: 50–59. https://doi.org/10.1016/j.clay.2007.04.008.

Kaufhold, S., R. Dohrmann, M. Klinkenberg, S. Siegesmund, and K. Ufer. 2010. "N2-BET Specific Surface Area of Bentonites." *Journal of Colloid and Interface Science* 349, no. 1: 275–282. https://doi.org/10.1016/j.jcis.2010.05.018.

Kaufhold, S., R. Dohrmann, D. Koch, and G. Houben. 2008. "The pH of Aqueous Bentonite Suspensions." *Clays and Clay Minerals* 56, no. 3: 338–343. https://doi.org/10.1346/CCMN.2008.0560304.

Kaufhold, S., M. Hein, R. Dohrmann, and K. Ufer. 2012. "Quantification of the Mineralogical Composition of Clays Using FTIR Spectroscopy." *Vibrational Spectroscopy* 59: 29–39. https://doi.org/10.1016/j.vibspec.2011.12.012.

Kaufhold, S., A. Kremleva, S. Krüger, N. Rösch, K. Emmerich, and R. Dohrmann. 2017. "Crystal-Chemical Composition of Dicoctahedral Smectites: An Energy-Based Assessment of Empirical Relations." *ACS Earth and Space Chemistry* 1, no. 10: 629–636. https://doi.org/10.1021/acsearthspacechem.7b00082.

Lagaly, G., and I. Dékány. 2013. "Colloid Clay Science." In *Developments in Clay Science, Handbook of Clay Science*, edited by F. Bergaya and G. Lagaly, 243–345. Elsevier.

Liu, C., H. Li, B. J. Teppen, C. T. Johnston, and S. A. Boyd. 2009. "Mechanisms Associated With the High Adsorption of Dibenzo-p-Dioxin From Water by Smectite Clays." *Environmental Science & Technology* 43, no. 8: 2777–2783. https://doi.org/10.1021/es802381z.

Lohmann, R., B. Vrana, D. Muir, et al. 2023. "Passive-Sampler-Derived PCB and OCP Concentrations in the Waters of the World—First Results From the AQUA-GAPS/MONET Network." *Environmental Science & Technology* 57, no. 25: 9342–9352. https://doi.org/10.1021/acs.est.3c01866.

Mader, B. T., K.-U. Goss, and S. J. Eisenreich. 1997. "Sorption of Nonionic, Hydrophobic Organic Chemicals to Mineral Surfaces." *Environmental Science & Technology* 31, no. 4: 1079–1086. https://doi.org/10.1021/es960606g.

Mayer, L. M. 1994. "Relationships Between Mineral Surfaces and Organic Carbon Concentrations in Soils and Sediments." *Chemical Geology* 114, no. 3–4: 347–363. https://doi.org/10.1016/0009-2541(94)90063-9.

Mayer, P., J. Tolls, J. L. M. Hermens, and D. Mackay. 2003. "Equilibrium Sampling Devices." *Environmental Science & Technology* 37, no. 9: 184A–191A. https://doi.org/10.1021/es032433i.

Meijer, S. N., W. A. Ockenden, A. Sweetman, K. Breivik, J. O. Grimalt, and K. C. Jones. 2003. "Global Distribution and Budget of PCBs and HCB in Background Surface Soils: Implications for Sources and Environmental Processes." *Environmental Science & Technology* 37, no. 4: 667–672. https://doi.org/10.1021/es025809l.

Organisation for Economic Cooperation and Development. 2000. *Test No. 106: Adsorption—Desorption Using a Batch Equilibrium Method*. Paris: OECD.

Ouyang, G., and R. Jiang. 2016. *Solid Phase Microextraction: Recent Developments and Applications*. Berlin Heidelberg: Springer.

Pan, B., P. Ning, and B. Xing. 2008. "Part IV—sorption of hydrophobic organic contaminants." *Environmental Science and Pollution Research* 15, no. 7: 554–564. https://doi.org/10.1007/s11356-008-0051-y.

Pašalić, H., A. J. Aquino, D. Tunega, G. Haberhauer, M. H. Gerzabek, and H. Lischka. 2017. "Cation–π Interactions in Competition With Cation Microhydration: A Theoretical Study of Alkali Metal Cation–Pyrene

Complexes." *Journal of Molecular Modeling* 23: 1–9. https://doi.org/10.1007/s00894-017-3302-3.

Pei, Z., J. Kong, X. Q. Shan, and B. Wen. 2012. "Sorption of Aromatic Hydrocarbons Onto Montmorillonite as Affected by Norfloxacin." *Journal of Hazardous Materials* 203: 137–144. https://doi.org/10.1016/j.jhazmat.2011.11.087.

Pérez-Botella, E., S. Valencia, and F. Rey. 2022. "Zeolites in Adsorption Processes: State of the Art and Future Prospects." *Chemical Reviews* 122, no. 24: 17647–17695. https://doi.org/10.1021/acs.chemrev.2c00140.

Poerschmann, J., Z. Zhang, F. D. Kopinke, and J. Pawliszyn. 1997. "Solid Phase Microextraction for Determining the Distribution of Chemicals in Aqueous Matrices." *Analytical Chemistry* 69, no. 4: 597–600. https://doi.org/10.1021/ac9609788.

Pohlert, T., G. Hillebrand, and V. Breitung. 2011. "Trends of Persistent Organic Pollutants in the Suspended Matter of the River Rhine." *Hydrological Processes* 25, no. 24: 3803–3817. https://doi.org/10.1002/hyp.8110.

Pouch, A., A. Zaborska, and K. Pazdro. 2018. "The history of hexachlorobenzene accumulation in Svalbard fjords." *Environmental Monitoring and Assessment* 190, no. 360. https://doi.org/10.1007/s10661-018-6722-3.

Qu, X., Y. Zhang, H. Li, S. Zheng, and D. Zhu. 2011. "Probing the Specific Sorption Sites on Montmorillonite Using Nitroaromatic Compounds and Hexafluorobenzene." *Environmental Science & Technology* 45, no. 6: 2209–2216. https://doi.org/10.1021/es104182a.

Sadri, S., B. B. Johnson, M. Ruyter-Hooley, and M. J. Angove. 2018. "The Adsorption of Nortriptyline on Montmorillonite, Kaolinite and Gibbsite." *Applied Clay Science* 165: 64–70. https://doi.org/10.1016/j.clay.2018.08.005.

Schlechtriem, C., L. Böhm, R. Bebon, H.-J. Bruckert, and R.-A. Düring. 2017. "Fish bioconcentration studies with column-generated analyte concentrations of highly hydrophobic organic chemicals." *Environmental Toxicology and Chemistry* 36, no. 4: 906–916. https://doi.org/10.1002/etc.3635.

Starek-Świechowicz, B., B. Budziszewska, and A. Starek. 2017. "Hexachlorobenzene as a Persistent Organic Pollutant: Toxicity and Molecular Mechanism of Action." *Pharmacological Reports* 69: 1232–1239. https://doi.org/10.1016/j.pharep.2017.06.013.

Steudel, A., and K. Emmerich. 2013. "Strategies for the Successful Preparation of Homoionic Smectites." *Applied Clay Science* 75: 13–21. https://doi.org/10.1016/j.clay.2013.03.002.

Strauss, R., G. W. Brümmer, and N. J. Barrow. 1997. "Effects of Crystallinity of Goethite: II. Rates of Sorption and Desorption of Phosphate." *European Journal of Soil Science* 48, no. 1: 101–114. https://doi.org/10.1111/j.1365-2389.1997.tb00189.x.

Tributh, H., and G. Lagaly. 1986. "Aufbereitung und Identifizierung von Boden-und Lagerstättentonen. II. Korngrößenanalyse und Gewinnung von Tonsubfraktionen: Fractionation of Clays and Soils and Identification of Clay Minerals. II. Particles Size Analysis and Preparation of Clay Subfractions." *GIT-Fachzeitschrift Für Das Laboratorium* 8: 771–776.

UBA. 2024. Nationale Trendtabellen für die deutsche Berichterstattung atmosphärischer Emissionen (Persistente Organische Schadstoffe, engl: POPs) 1990 - 2022: National Trend Tables for the German Atmospheric Emission Reporting (Persistent Organic Pollutants) 1990 - 2022. Umweltbundesamt, Dessau.

United Nations Environment Programme. 2020. "Stockholm Convention on Persistent Organic Pollutants (POPs), Text and Annexes Revised in 2019." http://www.pops.int/Portals/0/download.aspx?d=UNEP-POPS-COP-CONVTEXT–2021.English.pdf.

Wiltschka, K., L. Neumann, M. Werheid, et al. 2020. "Hydrodechlorination of Hexachlorobenzene in a Miniaturized Nano-Pd (0) Reaction System Combined With the Simultaneous Extraction of all Dechlorination Products." *Applied Catalysis B: Environmental* 275: 119100. https://doi.org/10.1016/j.apcatb.2020.119100.

Wiltschka, K., C. Wolkersdorfer, R. A. Düring, and L. Böhm. 2023. "Between Underground and the Deep Blue Sea: Contamination of Mine Water Effluents by Polychlorinated Biphenyls (PCBs)." *ACS ES&T Water* 3, no. 11: 3474–3484. https://doi.org/10.1021/acsestwater.3c00179.

Zhang, R., L. Zeng, F. Wang, X. Li, and Z. Li. 2022. "Influence of Pore Volume and Surface Area on Benzene Adsorption Capacity of Activated Carbons in Indoor Environments." *Building and Environment* 216: 109011. https://doi.org/10.1016/j.buildenv.2022.109011.

Zhang, Z., and J. Pawliszyn. 1993. "Headspace Solid-Phase Microextraction." *Analytical Chemistry* 65, no. 14: 1843–1852. https://doi.org/10.1021/ac00062a008.

Supporting Information

Additional supporting information can be found online in the Supporting Information section.